

Anne, please just look this over and see if it's  
OK. —CINDY

## POSITION REPEATABILITY OF SPECTRA OBTAINED WITH THE FOS

R.W. Lyons, E.A. Beaver, R.D. Cohen, V.T. Junkkarinen  
*Center for Astrophysics and Space Sciences*  
*University of California, San Diego*

Instrument Science Report CAL/FOS-111  
February 25, 1994

### Abstract

A number of sources of error have been suggested to explain the differences between the expected and actual wavelengths measured for specific features in FOS spectra. In this report, we use the sky observations made during Science Verification to determine the errors that might be expected due to non-repeatability of the aperture and filter-grating wheel position. The analysis was complicated by an unexpected problem with the GIM correction that will lead to an error in the zero point for every observation which uses the PODPS GIM correction software.

The peak-to-peak position variation for the G160L with the Blue tube is about 2 quarter steps; the value for the Red tube is about 4 quarter steps. The peak-to-peak variation for the G650L with the Red tube is about 6 quarter steps, but the features compared are much weaker and so less reliable.

Two modifications to the GIM correction as implemented in the PODPS reduction software are suggested.

### Introduction

3CR 286 is a QSO with a damped Ly $\alpha$  line present in the UV spectrum. In 1991, a low dispersion spectrum was obtained through the target acquisition aperture using the FOS G160L grating with the Red digicon. No wavelength calibration spectra were taken. The spectrum was reduced to flux versus wavelength in the standard manner for HST data. The measured wavelength for the damped Ly $\alpha$  line was about 10 Å away from where it had been expected based on the redshift of the 21 cm absorption. Since errors in the wavelength calibration and the internal-external offsets (compensation for the different optical paths for targets and calibration lamps) are expected to be small, this difference seemed rather large.

Uncertainties in the wavelength scale can be reduced by taking comparison spectra before and

after the exposure as is often done in ground-based work. While this is recommended for precision work, it is not normally done for FOS observations. Instead a standard calibration is applied to provide the correspondance between detector readout position (pixel number) and wavelength. The applicability of the standard calibration rests on the consistency with which the hardware can place (and hold) spectra in the same place on the detector's diode array, exposure after exposure. Inconsistency will cause the zero point of spectra to wander. The 10 Å error for 3CR 286 corresponds to a positioning error of about 1.5 diodes. The size of this error prompted an examination of the possible sources of wavelength error.

If we accept that the wavelength calibration error is small, then the errors should depend on the hardware repeatability. In this regard, there are a few areas that need to be considered. These are:

- 1) geomagnetically induced motion (GIM)
- 2) target centering error
- 3) aperture wheel non-repeatability
- 4) filter-grating wheel non-repeatability
- 5) other.

Early work with the FOS showed that an interaction between the Earth's magnetic field and the detectors caused the spectral image in the detector plane to wander. This geomagnetically induced motion due to incomplete shielding is about 2.95 diodes Gauss<sup>-1</sup> for the Red tube and about 0.7 diodes Gauss<sup>-1</sup> for the Blue tube. The effect is well understood (Baity *et al.* 1993), and routines for its removal have been incorporated into the PODPS reduction software.

The only observational source of error occurs in target centering. This error, target or perhaps observation dependent, can be systematic or random depending on the nature of the problem. The error in a target acquisition ranges from 1 - 2 quarter steps (Caganoff *et al.* 1992).

In general, tests indicate that the aperture wheel position repeats well and that problems here are not significant (Harms and Dressel 1992).

The largest source of hardware error is thought to be filter-grating wheel non-repeatability (Hartig 1989), however no on-orbit tests have been made. Non-repeatability would produce random zero point shifts in all observations. Errors here may have a configuration or time dependent component; the same could be true for the aperture wheel.

Sky spectra taken during Science Verification form a consistent data set that can be used to look for hardware variations. Since the sky uniformly fills the aperture, comparisons of sky spectra will not be affected by centering errors that might be present with discrete targets. Since the target acquisition aperture was used, the diode illumination will be insensitive to any geomagnetically induced motion perpendicular to the array. The output from the low dispersion configurations used in these tests contain well-defined zero order features and atmospheric emission lines whose positions can be reliably compared from spectrum to spectrum. If the GIM adjustments have been made correctly, these comparisons should provide a good estimate of the position errors due to both the aperture wheel and the filter-grating wheel. It is not possible to determine the

separate errors with these tests.

## Observations

Between 1991 and early 1992, a number of observations were made under Science Verification tests 2965, 2966 and 2967 to determine the FOS sky background. The G160L was used with the Blue detector for 70 runs; the Red detector was used with the G160L, G650L and prism on 68 runs. During each run, three sets of exposures (one file for each set) were made with each configuration tested. In this study, only the first sub-exposure from each run was used for each configuration – information from subsequent sub-exposures should be redundant because the hardware configuration was not changed. All of the observations were made with the target acquisition aperture and done in the ACCUM mode. The spectra were sampled at one-quarter diode intervals to improve the resolution. Interested readers should refer to Lyons *et al.* (1992, 1993) for further information about the sky data.

Only the output from the G160L and the G650L configurations include zero order spectra (the prism spectra have no line-like features which are regularly present). These features could be compared in the GIM corrected PODPS output but do not appear because there is no flux or wavelength calibration in this region. (Instead of using the zero order spectra, the geocoronal Ly $\alpha$  emission line could be substituted in the G160L Blue spectra. If this were done, a number of science observations could also be included in the analysis.) For the G160L and G650L configurations, the first file in each run was reduced with the FOS team's IDL CALFOS routines and a dummy, uniform IVS function. The newly reduced files were GIM corrected and included the zero order features. For each observation, CALFOS also produced a file containing the values of the magnetic field along the array axis,  $B_{eff} X$ , for each sub-exposure. The CALFOS sign convention is opposite that used by Junkkarinen *et al.* (1992).

The data discussed here can only be used to test the G160L and G650L configurations and, strictly speaking, only applies to the period from 1991 to early 1992.

## Analysis

Runs affected by discrete objects present in the target fields were identified by examining the profiles of the zero order features. In Figure 1, the bottom spectrum is the zero order spectrum from a typical sky exposure with no strong discrete sources. It has the rectangular profile (48 pixels FWHM) expected from the target acquisition aperture. The top spectrum has a much higher count rate and is sharply peaked (similar to the HST point spread function) because a discrete source was present, but off center, in the aperture. The sky contribution is actually the low wing (to higher pixel numbers) at a count rate of  $\sim 0.5$  counts  $\text{sec}^{-1}$   $\text{pixel}^{-1}$ . Both examples are from the G160L data obtained with the Blue detector. Runs affected by discrete objects were not included in the data sets used in this analysis.

For each configuration, a spectrum was chosen against which the others could be compared. The runs for each configuration were processed as necessary. For each run, the sum of the squares of the pixel-by-pixel differences between the zero order spectrum of the standard and the zero order spectrum of the first sub-exposure was determined at a number of different relative displacements (pixel shifts). A least squares parabolic fit about the minimum difference (i.e. the best match) was used to determine the displacement from the zero order spectrum of the standard. A brief discussion of the uncertainties involved in this correlation method is presented in the Appendix.

## Discussion

### Preliminary Results

As the HST orbits the Earth, it travels through a magnetic field whose strength is dependent on the telescope's position. Along the FOS diode array axis the strength,  $B_{eff} X$ , ranges from  $-0.3$  to  $0.3$  Gauss.

The small GIM factor for the Blue Digicon,  $0.7$  diodes  $\text{Gauss}^{-1}$ , corresponds to a shift range of  $\sim \pm 0.2$  diodes or about  $\pm 1$  quarter steps. The raw (uncorrected for GIM) G160L Blue spectra were correlated. The results are presented in Figure 2a. (In this and subsequent figures, there are two graphs. In the top graph, the results are presented chronologically by spectrum number. Note that the runs were not spaced uniformly in time. The results for the standard spectrum are indicated by a filled circle.) The peak-to-peak variation, 2 quarter steps, is in line with expectations from GIM considerations alone. The standard deviation ( $\sigma$ ) for these measurements is  $0.56$  quarter steps. The repeatability on the Blue side appears to be very good. A plot of the results against  $B_{eff} X$  shows no apparent correlation with the magnetic field. It was expected that the scatter would be smaller if the wander produced by the geomagnetic interaction were removed, so the observations reduced with CALFOS were correlated. While the results for the individual files are different (Figure 2b), the standard deviation unexpectedly is worse. In addition, the measured displacements are now strongly correlated with the magnetic field along the array axis, something that had not been evident with the raw data.

The G160L Red data were treated similarly - first the raw data were correlated (Figure 3a), then the CALFOS reduced data (Figure 3b). The scatter is essentially unaffected by the reduction. In this case, however, both sets of displacements are strongly correlated with magnetic field, although in the opposite sense.

The raw G650L Red data (Figure 4a) showed more scatter and a slightly larger range than the G160L Red data. This may have happened because the G650L zero order spectra are much weaker, in most cases containing fewer than  $10$  counts  $\text{pixel}^{-1}$ . (In the figures for the G650L data, results for runs in which the zero order spectrum averaged less than  $4$  counts  $\text{pixel}^{-1}$  are plotted as open circles.) The CALFOS reduced data are shown in Figure 4b. The scatter is unaffected by the reduction and the results are still correlated with the magnetic field.

## Why Didn't the Reduction Improve Things?

The GIM correction did not improve the results. In fact, in the case of the Blue detector results, a correlation with the magnetic field was introduced that was not apparent in the raw data. Something was clearly wrong – the data appeared to have been over-corrected. Before proceeding farther, the values and correct application of the GIM factors were checked.

We offer the following explanation for the over-correction. Each data set was formed from a series of totally independent observations. At the time these observations were made, each FOS observation was preceded by a de-perm (Hartig *et al.* 1991 terminology) or degauss (Baity *et al.* 1993 terminology). Since only the first readout in each observation was measured, each readout used had been preceded by a degauss. Previously, using the Red detector, Hartig *et al.* (1991) had determined different GIM factors from observations using the calibration lamp and observations mapping the target acquisition aperture using the LED. The GIM factor was smaller for the calibration lamp exposures where all the readouts were preceded by a degauss. For the Red side, this smaller factor, later confirmed in laboratory tests (Beaver and Foster 1992), was  $\sim 1.8$  diodes Gauss<sup>-1</sup>. The GIM coefficients currently used in CALFOS (and PODPS) were derived from the target acquisition maps. In these, only the first readout is preceded by a degauss. Similar tests were not run on the Blue side where the shielding is thought to be better by a factor of 4 or so. Under this assumption, the factor for the Blue side is somewhere around 0.4 diodes Gauss<sup>-1</sup>.

In practice, any given observation may be broken into several exposures each of which may have many sub-exposures carried out in ACCUM or RAPID-READOUT mode. From the user standpoint, each exposure has a unique file name. If a degauss operation is run prior to each exposure, the wavelength zero points for files reduced with the standard reduction package will be different. The sizes of the differences will depend on the differences in the initial values of  $B_{eff}$  X. This may lead to registration errors when files are combined. In addition, the wavelength scale may be offset because the wavelength zero point for the observation is not the same as that used in the standard wavelength calibration.

## Final Results

The results for the Blue tube were acceptable without making any GIM corrections. The results for the lower GIM factor are shown in Figure 2c. Because the software only applies integral pixels shifts, only one run was affected when the lower factor was used.

The results for the Red spectra obtained with the G160L improved when the smaller GIM correction factor, 1.80 diodes Gauss<sup>-1</sup>, was used, but some correlation with magnetic field still remained (Figure 3c). The scatter is higher than the Blue tube's for the same configuration by almost a factor of 2. Since both detectors see the same aperture configuration at each aperture position (the apertures are paired), the aperture wheel can be ruled out as the source of this discrepancy. Some discrepancies in ground-based testing had resulted from the use of different filter-grating wheel motors on the two sides (Hartig 1989), but both sides now use the same motor (Hartig, priv. comm.). The repeatability of the filter-grating wheel position cannot be ruled out however. While the same dispersive element is used in both data sets, the position of the filter-

grating wheel is different for each detector. There are several other known factors which have not been taken into account but which may be contributing to the discrepancy. In an unpublished study of test ET 3138 run on the Red side, Hartig *et al.* (1991) found that the GIM factors varied by about 8% depending on the orientation. In addition, they found some evidence for a position drift, perhaps due to a temperature dependence. Some of the scatter may be due to differences in the instrument warm-up time (Lindler and Bohlin 1984). Long term factors may be involved.

The results (Figure 4c) improved for the G650L data taken with the Red tube. The results improved further when those spectra with average count rates below 4 counts pixel<sup>-1</sup> (about 20 spectra) were ignored. The additional improvement was small, however, because the values from the poorer exposures were scattered throughout the range of the better data rather than being concentrated at the extremes. The results still show a larger scatter than those obtained with the G160L on the Red side.

The results for the different configurations are presented in Table I. The first order coefficient of a linear least squares fit relating the displacements to  $B_{eff} X$  is indicated for the different G160L options. Note that the units for these coefficients are quarter steps Gauss<sup>-1</sup> not diodes Gauss<sup>-1</sup> as used elsewhere in the text. Based on the raw data used here, the GIM factors, for exposures immediately preceded by a degauss, should be about 0.2 diodes Gauss<sup>-1</sup> for the Blue detector and 1.4 diodes Gauss<sup>-1</sup> for the Red detector.

## Conclusions and Recommendations

### GIM Software Correction

- 1) We have no clear evidence that any significant GIM correction should be applied to Blue spectra taken immediately after a degauss. The results presented here indicate that the Blue side may be a factor of 8 or so better than the Red side, as opposed to the factor of 4 normally assumed. A test similar to ET 3138, run for the Red side, should be considered for the Blue side to verify the sizes of the GIM factors.
- 2) The GIM corrections were originally implemented to register the sub-exposures within a given exposure, which they do. However, the manner of implementation has not corrected the lack of registration between exposures. The PODPS GIM reduction procedure should be changed to take into account the existence of two GIM correction factors - one for data taken right after a degauss and another for subsequent data. The FOS team's IDL program, CALFOS, should be modified similarly. (A word of caution here. During 1991, a new keyword, CCS7, was added to the header files. This keyword points to a file that has the current GIM parameters in it.)
- 3) The GIM correction software makes corrections in integral pixel shifts. The small coefficient on the Blue side means that, in certain cases, the application of the GIM correction further degrades the resulting spectra. We recommend modifying the software to allow sub-pixel shifts at least on the Blue side.

4) The FOS wavelength calibrations and internal-external offsets need to be reassessed in light of the presence of two GIM factors. Flat fields and intensity calibrations may also need some minor tuning.

### Repeatability

1) Experiments to determine the reasons for the differences between the Red and Blue detector results should be conducted in the hopes of improving the quality of the Red detector data. Perhaps, these are due solely to the filter-grating wheel positioning. On the other hand, they may be due to some other factor(s) to which the Red tube is more sensitive.

2) For a random observation, the maximum difference in the zero point due to non-repeatability of the target aperture and the G160L position of the filter-grating wheel is about 2 quarter steps for the Blue tube and 4 quarter steps for the Red tube. The difference is about 6 quarter steps for the G650L with the Red tube.

3) For a random set of observations, we derive an uncertainty ( $1\sigma$ ) in the target aperture and G160L position on the filter-grating wheel of 0.5 quarter steps for the Blue detector and 0.8 quarter steps for the Red detector. The uncertainty for the G650L with the Red tube is about 1.4 quarter steps.

4) Provisions should be made to monitor the long term performance of the aperture/filter-grating wheel combination. Because of the layout of the filter-grating wheel, it should be possible to use science observations to monitor some combinations. Geocoronal Ly $\alpha$  can be used with the G130H and G160L configurations on the Blue side. These filter-grating wheel positions correspond to the G780H and G270H configurations on the Red side. When smaller apertures are regularly in use with COSTAR, the zero order features in observations with the G160L on the Red side will help pin down the repeatability of that configuration as well as the G270H on the Blue side. (The smaller apertures are needed to reduce the impact from target centering errors.) At the moment, running repeatability tests with the Blue side is preferable because it is less sensitive to magnetic field effects. The GIM factors need to be verified however. Tests on other configurations, especially the high dispersion ones, should be considered.

5) FOS observations are currently being run with real-time GIM corrections and no degaussing. We recommend that the stability of the zero point of the wavelength scale be monitored.

## Future Work

- 1) Some preliminary lab work has indicated that the value of  $B_{eff}$  X experienced by the Digicon may be affected by some other components in the instrument.
- 2) The question of possible temperature dependencies needs to be examined.
- 3) It is possible that enough exposures have already been made with the G130H to place some limits on the performance of this configuration by using the position of the geocoronal Ly $\alpha$  line. Calibration spectra may be used for the other configurations. Care should be taken to avoid comparing spectra taken with the on-board GIM correction activated and those taken without it.

## Acknowledgements

The authors wish to thank George Hartig for help in clarifying some of the points made in the text.

The authors gratefully acknowledge the support of NASA Contract NAS5-29293 and NASA Grant NAG5-1630.

## References

- Baity, W.A., Beaver, E.A., Cohen, R.D., Junkkarinen, V.T., Lyons, R.W., Fitch, J.E., Hartig, G.F., Lindler, D.J., "Performance of the FOS detectors in a variable external magnetic field", in *SPIE Proc 1945: Space Astronomical Telescopes and Instruments II*, ed P.Bely, J.Breckinridge (SPIE: Bellingham), 1993.
- Beaver, E.A., Foster, P., "Lab Test Results of the FOS Detector Performance in a Variable External Magnetic Field", FOS Instrument Science Report CAL/FOS-082, March, 1992.
- Caganoff, S., Tsvetanov, Z., Armus, L., "FOS Onboard Target Aquisition Tests", FOS Instrument Science Report CAL/FOS-081, March, 1992.
- Lindler, D., Bohlin, R. "High Voltage Settle (FOS Calibration #8)", FOS Instrument Science Report CAL/FOS-010, December, 1984.
- Lyons, R.W., Baity, W.A., Beaver, E.A., Cohen, R.D., Junkkarinen, V.T., Linsky, J.B., Bohlin, R.C., "Faint Object Spectrograph on-orbit sky background measurements", in *SPIE Proc 1945: Space Astronomical Telescopes and Instruments II*, ed P.Bely, J.Breckinridge (SPIE: Bellingham), 1993.



Lyons, R.W, Baity, W.A., Beaver, E.A., Cohen, R.D., Junkkarinen, V.T. Linsky, J.B., "Faint Object Spectrograph On-Orbit Sky Background Measurements ", FOS Instrument Science Report CAL/FOS-083 (preliminary), August, 1992.

Harms, R. Dressel, L., "Aperture Calibrations During Science Verification of the FOS", FOS Instrument Science Report CAL/FOS-072, (report being rewritten - results quoted are from the FOS Science Verification Report Summary), July, 1992.

Hartig, G, "FOS Filter-Grating Wheel Repeatability: Dependence on Motor Selection", FOS Instrument Science Report CAL/FOS-060, May, 1989.

Hartig, G., Lindler, D., Beaver, E., Junkkarinen, V., Lyons, R., "FOS Red-Side Sensitivity to the Geomagnetic Field", FOS Instrument Science Report (unnumbered), May, 1991.

Junkkarinen, V.T., Beaver, E.A., Cohen, R.D., Hier, R., Lyons, R., Rosenblatt, E., "Geomagnetic Image Deflection Problem in the Faint Object Spectrograph", FOS Instrument Science Report CAL/FOS-066, April, 1992.

Table I: Result of 0 Order Sky Spectrum Correlation

	$\sigma$ (qs*)	Peak-to-Peak (qs*)	Linear Fit Slope (qs* Gauss <sup>-1</sup> )
G160L Blue - 64 Spectra standard - Y0G10N01T			
Raw Data	0.47	2.1	0.67
GIM = 0.7 diodes Gauss <sup>-1</sup>	0.72	3.5	3.28
GIM = 0.4 diodes Gauss <sup>-1</sup>	0.47	2.1	0.90
alternate standard - Y0G32501T			
Raw Data	0.44	2.1	0.60
G160L Red - 62 Spectra standard - Y0G12401T			
Raw Data	1.19	5.3	-5.81
GIM = 2.95 diodes Gauss <sup>-1</sup>	1.22	5.8	6.01
GIM = 1.80 diodes Gauss <sup>-1</sup>	0.83	4.1	1.33
G650L Red - 62 Spectra standard - Y0G11W04T			
Raw Data	1.69	8.1	-6.23
GIM = 2.95 diodes Gauss <sup>-1</sup>	1.69	7.2	5.50
GIM = 1.80 diodes Gauss <sup>-1</sup>	1.40	5.9	1.02
weak sub-exposures rejected			
GIM = 1.80 diodes Gauss <sup>-1</sup>	1.27	5.2	1.93

\* = qs stands for quarter steps  $\sim 12.5\mu$  (one diode is  $50\mu$ )

## Appendix - Correlation Errors

There are several sources of variation in the correlation procedure applied in this analysis. The main ones are:

- 1) poor standard (noisy or not representative)
- 2) variations in the profiles of the features being measured
- 3) poor fit to the correlation values.

The standards chosen are thought to be representative of the data in the sense that they have the same profile. Observations whose target fields had an obvious discrete point source present were not considered. Weak sources may have been present in the standard spectra. These should not have much affect on the results. In order to test the suitability of the standard and to determine the errors that might be expected, the raw G160L Blue spectra were correlated with two standards. The standard used for the analysis was Y0G10N01T. The zero order for this file is shown in the lower plot of Figure 1. The second standard was Y0G32501T which had an average count rate of  $1.2 \text{ counts sec}^{-1} \text{ pixel}^{-1}$  or about 3 times higher. The peak-to-peak range and the variation ( $\sigma$ ) about the mean value are almost the same as those found for the results with Y0G10N01T. The linear fit is a bit better. When the displacements were compared, the peak-to-peak variation for the difference in the displacement for a given readout was 1 quarter step and the standard deviation for the 64 differences was 0.2 quarter steps.

Variations in the profiles of the features being measured should not be a serious problem with this data since the observations whose target fields were not free of discrete objects were removed. Weak sources may still be present or lost in the noise. These sources should not have a strong impact on the results unless they affect the edges of the zero order features since it is these regions which dominate the correlation.

This program fits the correlation values with a least squares parabolic fit. The best correlation occurs at the displacement where the tangent to the parabola fit is parallel to the x axis. Since the zero order profile should be fairly repeatable, the parabola fit should be fairly symmetric (in cases of asymmetry, the best fit position will be a function of the number of points actually used to fit the parabola and can be used to select core or wing line fits). There is only one parameter in this fit - the number of points that are fit. This can be important when the profiles are noisy since this will lead to noisy correlation values. For the G160L data 9 correlation values symmetrically placed about the minimum correlation value were fit. (Since the profiles are about 48 pixels wide at the half depth, the correlation values will show some variation over a range of at least 96 displacement steps.) The procedure was repeated for the G160L Blue data using a 17 point fit. The peak-to-peak difference in corresponding measurements was 0.8 quarter steps and the standard deviation for the 64 differences was 0.15 quarter steps. The fit procedure for the G650L data used 19 points because the weak zero order features resulted in noisy correlation functions.

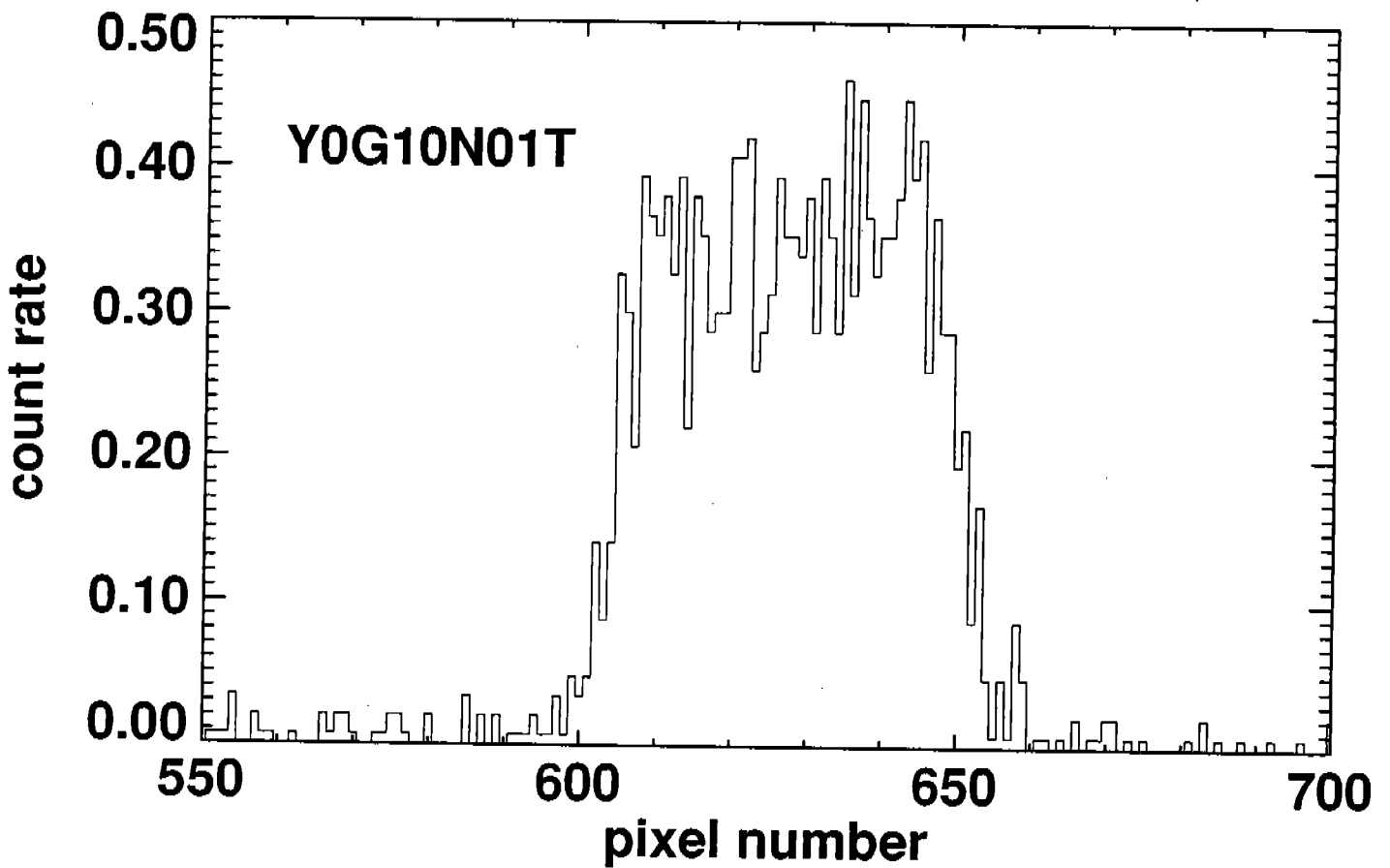
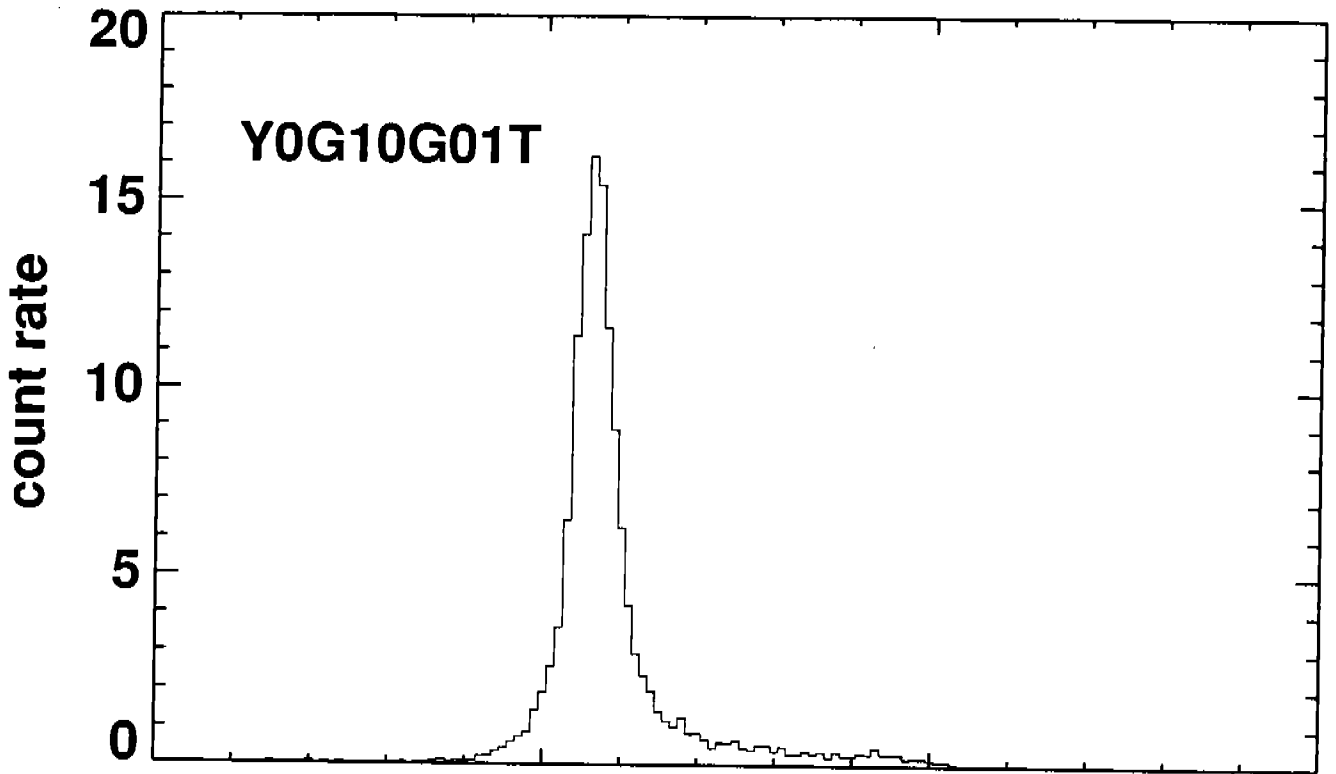
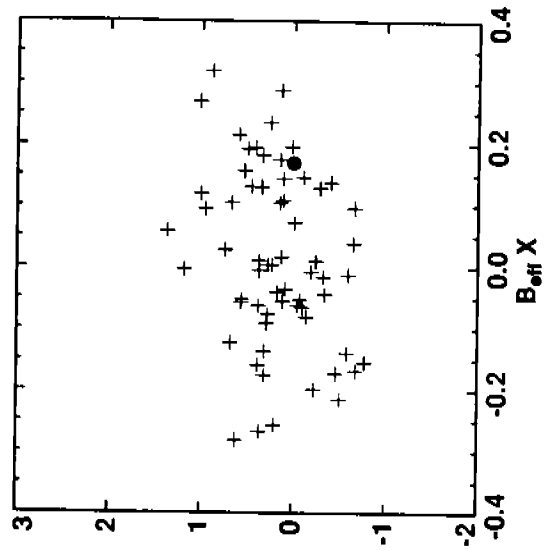
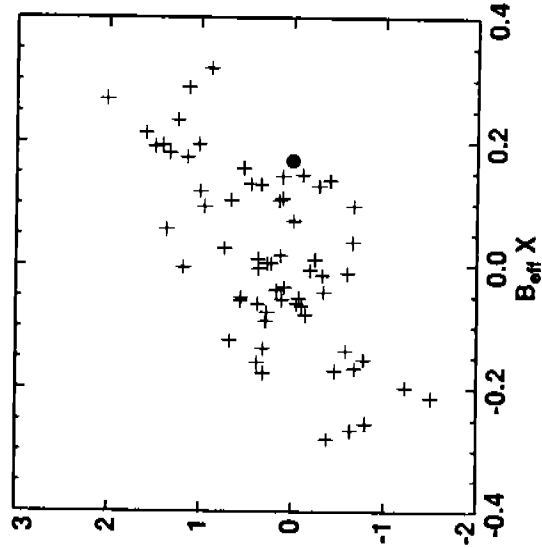
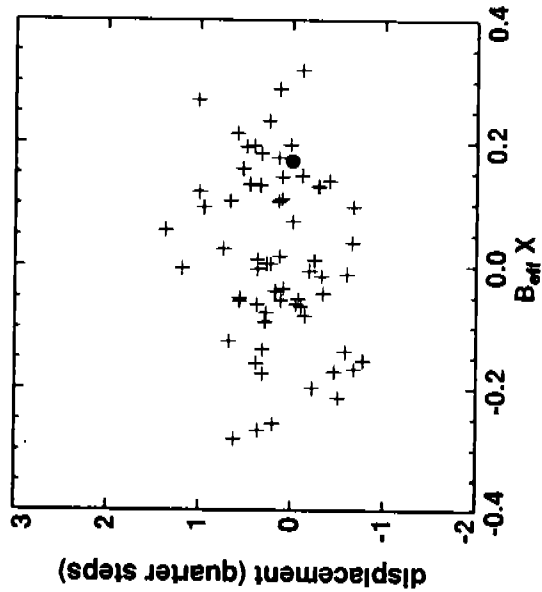
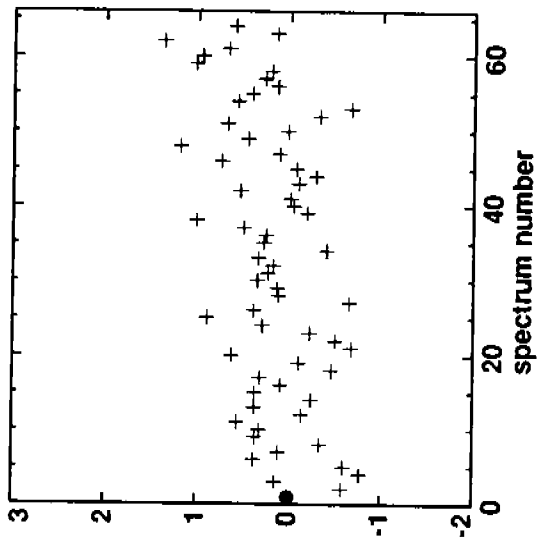
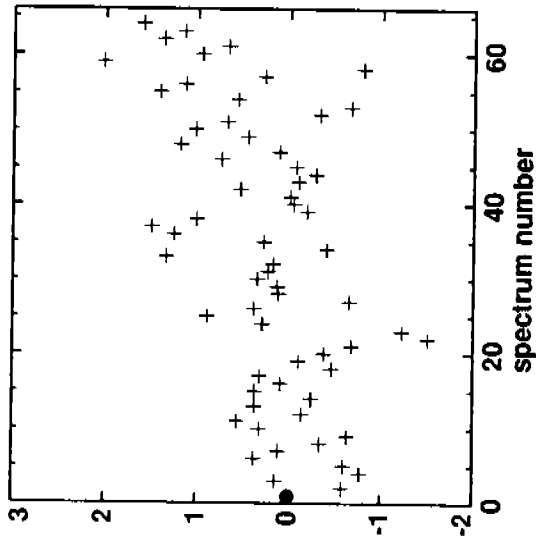
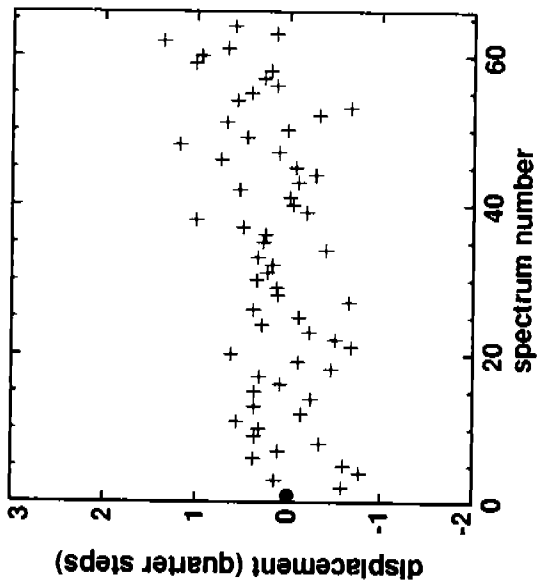


Fig. 1: G160L - Blue - 0 Order Sky Spectra

Figure 2: G160L and Blue Detector

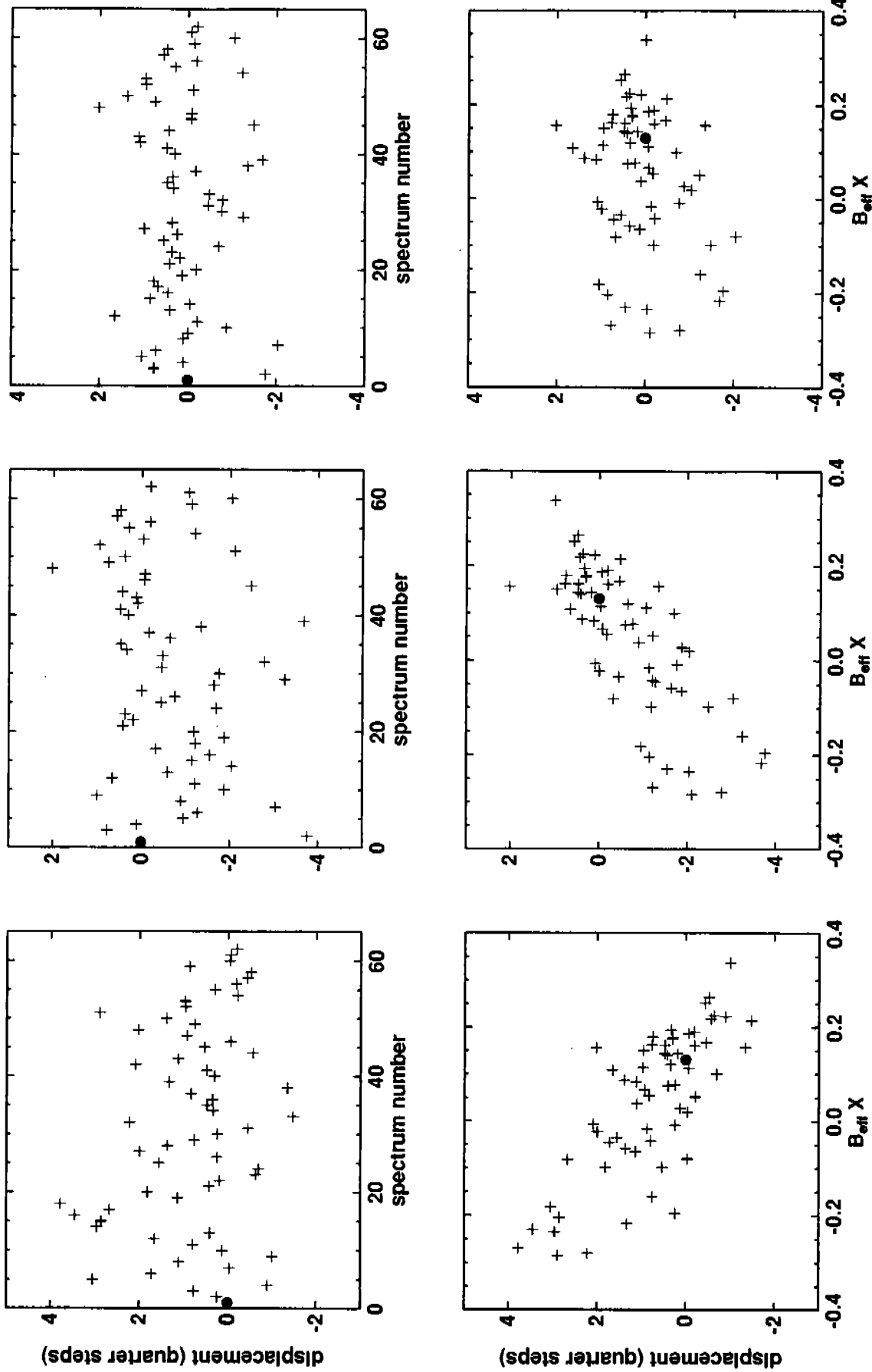


2a) - Raw Spectra

2b) GIM Coefficient = 0.7 Diodes Gauss<sup>-1</sup>

2c) GIM Coefficient = 0.4 Diodes Gauss<sup>-1</sup>

Figure 3: G160L and Red Detector

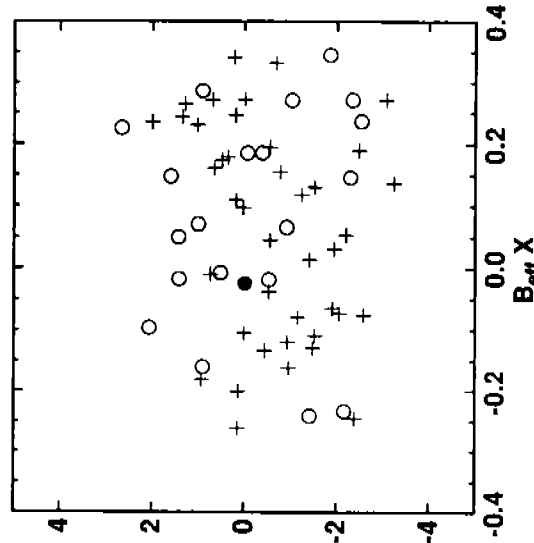
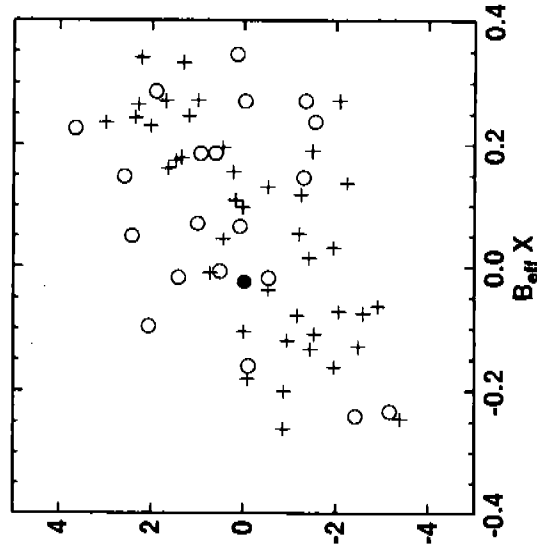
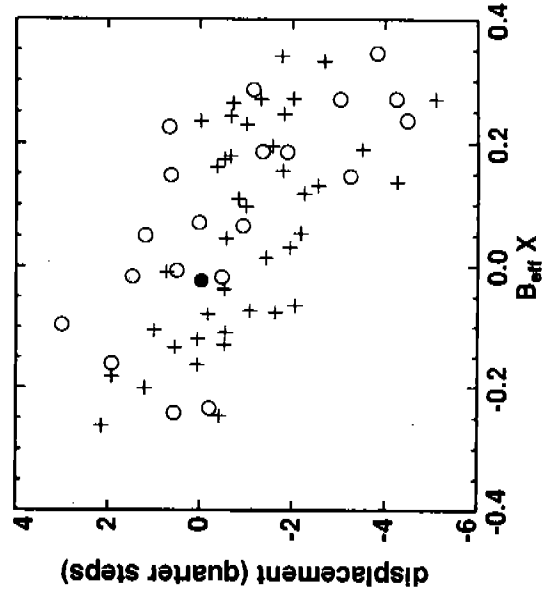
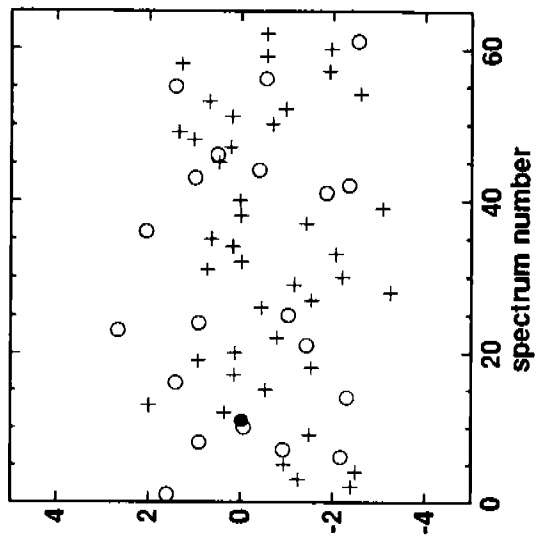
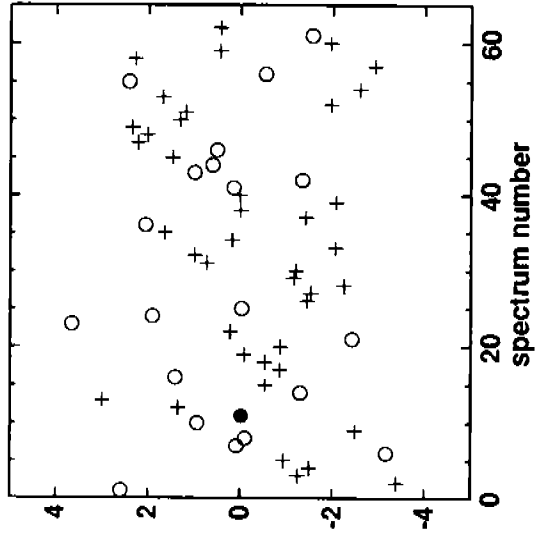
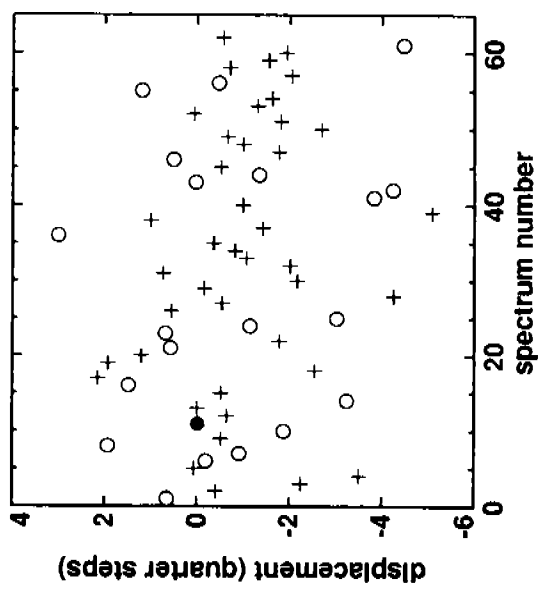


3a) Raw Spectra

3b) GIM Coefficient = 2.95 Diodes Gauss<sup>-1</sup>

3c) GIM Coefficient = 1.80 Diodes Gauss<sup>-1</sup>

Figure 4: G650L and Red Detector



4a) Raw Spectra

4b) GIM Coefficient = 2.95 Diodes Gauss<sup>-1</sup>

4c) GIM Coefficient = 1.80 Diodes Gauss<sup>-1</sup>

